International Immunopharmacology 75 (2019) 105779

Contents lists available at ScienceDirect

International Immunopharmacology

journal homepage: www.elsevier.com/locate/intimp

SIRT1-regulated HMGB1 release is partially involved in TLR4 signal transduction: A possible anti-neuroinflammatory mechanism of resveratrol in neonatal hypoxic-ischemic brain injury

Kai Le[a,b], Enkhmurun Chibaatar Daliv[a,b], Shanshan Wu[a,b], Fangyuan Qian[a,b], Abdoulaye Idriss Ali[a,b], Dafan Yu[a,b], Yijing Guo[a,*]

[a] Department of Neurology, Affiliated Zhongda Hospital of Southeast University, Nanjing, Jiangsu Province 210009, China
[b] School of Medicine, Southeast University, Nanjing, Jiangsu Province 210009, China

ARTICLE INFO

Keywords:
Hypoxic-ischemic brain injury
Resveratrol
Microglia
HMGB1
TLR4
SIRT1

ABSTRACT

Neonatal hypoxic-ischemic brain injury (HIBI) is a knotty disease that lacks appropriate treatment. Inflammation is an important contributor to brain damage, and microglia are responsible for eliciting early and pronounced inflammatory reactions in the immature brain after hypoxic-ischemic (HI) insult. Acetylated HMGB1 can be released from immune cells into the extracellular space, where it acts as a danger-associated molecular pattern molecule to activate TLR4 signalling-mediated inflammatory responses. Resveratrol has neuroprotective and anti-inflammatory effects against HIBI, but whether these effects involve the regulation of the TLR4 signalling pathway and whether HMGB1 participates in this process is still unclear. We investigated the anti-inflammatory effects of resveratrol in HIBI and the molecular mechanisms potentially involved in the effect. The *in vivo* and *in vitro* results indicated that the level of cytoplasmic HMGB1 in microglia increased after insult and that treating experimental animals or mouse BV2 microglial cells with resveratrol attenuated HI insult-induced neuroinflammation, which was characterized by improved behavioural defects, reduced microglial activation and TLR4/MyD88/NF-κB signalling, and attenuated primary neuronal damage; this was accompanied by the inhibition of HMGB1 nucleoplasmic transfer and extracellular release. EX527 pretreatment reversed these effects. In addition, co-immunoprecipitation confirmed that SIRT1 was directly involved in the HMGB1 acetylation process in BV2 cells after oxygen glucose deprivation. These data demonstrate that resveratrol plays a neuroprotective role in neonatal HIBI by activating SIRT1 to inhibit HMGB1/TLR4/MyD88/NF-κB signalling and subsequent neuroinflammatory responses.

1. Introduction

Neonatal hypoxic-ischemic encephalopathy (HIE), or hypoxic-ischemic brain injury (HIBI), is caused by cerebral blood flow and oxygen supply disorders and is the most common cause of perinatal brain injury, which may lead to neonatal death or cause irreversible and lifelong mental and physical disabilities, including epilepsy, cerebral palsy [1], and cognitive dysfunction. Currently, the incidence of this disease is relatively high. Although therapeutic hypothermia provides neuroprotection, the improvement in outcomes has been modest, as up to half of treated neonates do not survive [2], and approximately 1/3 to 1/2 of patients exhibit persistent neurologic abnormalities or low IQ at 6 to 7 years of age [3,4]. Severe sequelae and the challenges of treating HIE cause global public health problems, placing a heavy burden on society and families. Therefore, more effective alternative or complementary therapies need to be developed.

Neuroinflammation is regarded as an important contributor to the pathogenesis of HIE. Many experimental studies have described the significant functions of immune cells in promoting brain injury and subsequent tissue repair and remodelling at various stages of the hypoxic-ischemic (HI) cascade [5–7]. The hallmark of brain neuroinflammation is the activation of microglia. As the resident innate immune cells of the brain, microglia, rather than infiltrating blood-derived macrophages, are responsible for eliciting early and pronounced inflammatory reactions in the immature brain after HI insult [8–10]. Numerous studies have demonstrated that stressed neurons can induce microglial activation and promote the release of pro-inflammatory cytokines, which contribute to ongoing secondary neuronal and

* Corresponding author.
E-mail address: guoyijingseu@126.com (Y. Guo).

https://doi.org/10.1016/j.intimp.2019.105779
Received 24 June 2019; Received in revised form 22 July 2019; Accepted 23 July 2019
Available online 27 July 2019

oligodendroglial injury [9,11,12]. To this end, alternative drugs that target the inhibition of the inflammatory reaction have been proposed as promising approaches for ameliorating deficits induced by HI insult.

Resveratrol (3,5,4′-trihydroxystilbene; RES) is a polyphenolic phytoalexin that is naturally found in various edible plants. A growing body of preclinical evidence suggests that RES has the potential to affect a variety of human diseases; it can prevent neuronal injury, reduce inflammation, and promote nerve repair and regeneration in a variety of experimental cerebral stroke models in adult rodents through different mechanisms [13–16]. In an animal model of neonatal HIBI, RES administration also plays a protective role, in which the strong inhibition of neuroinflammation is considered an important factor [17]. Although the anti-inflammatory mechanism of RES in cerebral stroke in the mature brain has been clarified, its specific mechanism in the treatment of neuroinflammation induced by HI insult in the immature brain is still largely unclear and requires further research.

High mobility group box-1 (HMGB1), a non-histone DNA binding protein with a highly conserved sequence that can be synthesized by almost all cells, was shown twenty years ago to be a pro-inflammatory cytokine and a late mediator of sepsis [18]. Since then, its important role in the inflammatory response has been gradually unveiled. HMGB1 is usually localized to the nucleus and, upon stimulation, enters the extracellular space, where it acts as a damage-associated molecular pattern (DAMP) molecule that binds to pattern recognition receptors such as Toll-like receptors (TLRs) [19] or receptors advanced glycation end products (RAGE) [20], thereby shifting the microglia to a pro-inflammatory phenotype [21] and promoting the secretion of various pro-inflammatory cytokines (such as IL-1 and TNF-α) [22]. As a pro-inflammatory factor, HMGB1 has been reported to be associated with the pathogenesis of various neurological diseases [23,24]; for example, its levels increase in the peripheral blood of neonates with HIE [25]. The goal of this study was to investigate whether HMGB1 is also involved in the inhibition of HI insult-induced neuroinflammation by RES and its potential mechanism.

Therefore, in the present study, we used the classic Rice-Vannucci [26] model to induce HIBI in neonatal mice and adopted oxygen glucose deprivation (OGD) treatment to simulate HI insult in microglial cells *in vitro*. Since acetylation is the main post-transcriptional modification of HMGB1, because previous studies have reported that the deacetylase activity of Sirtuin 1 (SIRT1) participates in the deacetylation of HMGB1 in acute kidney injury [27], and because RES is recognized as a SIRT1 activator, we attempted to explore the anti-neuroinflammatory mechanism of RES in HIBI in neonatal mice from the perspective of the HMGB1-TLR4 axis and investigated whether SIRT1 is involved in this mechanism.

2. Materials and methods

2.1. Experimental animals and hypoxic-ischemic brain injury induction

Timed-pregnant ICR mice were purchased from the Animal Core Facility of Nanjing Medical University and housed under standard conditions (21–24 °C, 12-h light–dark cycle) in specific pathogen-free animal quarters with unlimited access to standard food and water. Postnatal day 7 (P7) littermate mice of both sexes were used in the experiment. Pups were randomly assigned to four groups, namely, the sham-operated control (sham) group, the HI + PBS group, the HI + RES group, and the HI + EX527 (a specific SIRT1 inhibitor) + RES group, with the same number of pups in each group.

The Rice-Vannucci method was used to establish HIBI with some modifications [28]. Briefly, P7 pups weighing 4.5 to 5.5 g were anaesthetized with isoflurane, the anterior midline of the neck skin was incised and the right common carotid artery was exposed. The proximal and distal ends were ligated separately, cutting off the blood from the middle artery, and the skin was sutured. The duration of the entire operation was limited to 5 min for each mouse. The pups were then returned to their dams for 2 h of recovery. Subsequently, the pups were placed in a hypoxia chamber (8% oxygen +92% nitrogen was continuously applied) with a heating pad of constant temperature (37 °C) for 1 h. The sham group underwent anesthesia and incision only. The animal experiments were performed in accordance with the International Guiding Principles for Animal Research provided by the Council for International Organizations of Medical Sciences. The Animal Ethical and Welfare Committee of Southeast University approved all animal experiments.

2.2. Drug administration of animals

RES and EX527 were purchased from MCE (MedChemExpress, Monmouth Junction, NJ, USA), and 10 mg/ml (RES) and 1 mg/ml (EX527) stock solutions were produced with dimethyl sulfoxide (DMSO). Based on the previous literature, the stock solutions were diluted with PBS to a concentration of 100 mg/ml (RES) [29] and 10 mg/ml (EX527) [30] for intraperitoneal injection. The drug was administered immediately after HI insult and 12 h later. Specifically, in the HI + RES group, RES only was given; in the HI + EX527 + RES group, EX527 was given first, and RES was injected 1 h later. Equal volumes of PBS were administered in the same manner to the sham group and HI + PBS group. According to the weight of the pups, the injection volume was estimated to be 45–55 μl/mouse.

2.3. Behavioural tests

To assess the effects of RES on the neurobehaviour of the study subjects, the following behavioural tests were used.

2.3.1. Cylinder test

We evaluated the asymmetry of forelimb use using the cylinder test two weeks after HI insult, according to a previously reported method [31]. Briefly, each mouse was individually placed in a transparent cylinder with a 14-cm inner diameter and a height of 30 cm and video recorded until it reared and touched the cylinder wall with its forepaw (s) > 20 times; this took approximately 3–5 min. The number of contacts with the cylinder wall by the left or right forepaw during this time was counted. The asymmetry of forelimb use and paw preference were calculated using the following formula: (right [non-impaired side]-left [impaired side])/ (left + right) × 100%.

2.3.2. Forelimb suspension experiment

A forelimb suspension experiment was conducted after the cylinder test. In short, a smooth glass rod with a diameter of 0.5 cm was placed on a shelf with a height of 45 cm. Sponge pads were laid below the glass rod. Each mouse was placed on the glass rod so that it gripped the rod with its forelimbs. Timing was started, and timing ended when the mouse fell. This experiment was used as a reflection of the muscle strength and motor coordination of mice. A shorter latency to fall represented worse muscle strength and motor coordination.

2.3.3. Open-field test

Spontaneous activity and exploratory behaviours were assessed in the open-field test three weeks after HI insult. The open-field test was performed using a white square open-field apparatus (40 × 40 × 45 cm) made of plastic permeable to infrared light. Infrared lights were mounted at specific intervals along the X, Y, and Z axes of the open-field arena. The area was divided into 16 square zones, of which the four central squares (25% of the total area) were considered the central zone. The animals were allowed to explore the open-field arena freely for 10 min in the light and for the next 5 min in the dark. Each evaluation index was recorded by a video tracking system (ANY-maze).

2.4. Histological examination

Hematoxylin-eosin (HE) staining was used to observe changes in histology, such as hippocampal and cortical morphology. The brains were paraffin-embedded and cut into 4 μm-thick coronal sections, which were then dewaxed with a series of xylene and alcohol. The sections were stained with hematoxylin and eosin, and histopathological changes were observed at 40× and 200× under an optical microscope.

2.5. Primary neuronal culture and BV2 microglial cell culture

Primary cultured murine cortical neurons were prepared from the cortex of P0 mice. Briefly, P0 mice were immersed in 75% ethanol for 5 min after anesthesia and killed by decapitation. The cortices from the isolated brains were carefully stripped of the blood vessels and meninges, dissected in pre-cooled HBSS and then digested in 1.25% trypsin (Gibco) at 37 °C for 20 min. The trypsin digestion was terminated by Dulbecco's modified Eagle's medium (DMEM)-F12 with 10% foetal bovine serum (FBS) (Gibco). The cell suspension was prepared by gently pipetting 20 times with a Pasteur pipette and allowed to stand for 2 min. The cell suspension was centrifuged at 1000 rpm for 10 min, and the supernatant was removed. The precipitate was resuspended in DMEM-F12 with 10% FBS, 1% 0.5 mmol/l glutamate (Sigma) and 1% penicillin/streptomycin (Gibco). After the debris was removed with a 70-μm nylon strainer, the cells were plated in 0.1 mg/ml poly-D-lysine-coated confocal dishes (1.0×10^5 cell/well). The medium was changed to Neurobasal-A medium (NBM; Gibco) supplemented with 2% B27 (Gibco), 1% 0.5 mmol/l glutamate and 1% penicillin/streptomycin after 6 h. Cytosine arabinoside (2.5 μg/ml) was added on the third day of culture to inhibit the excessive proliferation of non-neuronal cells and discarded after 24 h. After that, half of the medium was replaced with new medium every 2 d, and the cultured cortical neurons were used for experiments on days 7–10.

Mouse BV2 microglia cells were donated by the School of Pharmacy of Nanjing Medical University and maintained in high glucose DMEM (Sigma) supplemented with 10% FBS, 4500 mg/l glucose and 1% penicillin/streptomycin. All cell cultures were maintained in a humidified incubator at 37 °C and 5% CO_2.

2.6. Cell viability and proliferation assays

Cell viability and proliferation assays were used to determine the optimal treatment conditions. BV2 cells were inoculated in quadruplicate in 96-well plates at a density of 1×10^4 cells per well for 24 h and then treated with different concentrations of RES or EX527 (5 μM, 10 μM, 25 μM, 50 μM, 100 μM, 150 μM and 200 μM) for 6 h, 12 h or 24 h or treated with OGD for different times (1 h, 2 h, 3 h, 4 h and 5 h). The concentration of DMSO was not > 0.1% to avoid cytotoxicity caused by DMSO. Then, 10 μl of CCK-8 reagent (APExBIO, Houston, USA) was added to each well, and the cells were incubated at 37 °C for 1 h. We used an automatic fluorescence microplate reader to measure the absorbance at 450 nm to obtain the optical density (OD) values for each well. Cell viability was calculated as follows: cell viability = $(OD_{treat} - OD_{blank})/(OD_{con} - OD_{blank})$.

2.7. OGD treatment of BV2 cells

Cells were pretreated with the indicated concentration of RES or EX527 (the optimal concentrations were determined by the CCK-8 assay) for 3 h and then washed 3 times with PBS. The normal culture medium was switched to DMEM without glucose and FBS, and then the cells were incubated in a hypoxia chamber with 1% O_2/5% CO_2/94% N_2 at 37 °C for the appropriate time. At the end of OGD treatment, the cells were reperfused by immediately changing the medium to normal medium with RES or DMSO and incubated for 12 h or 24 h under normal conditions for subsequent experiments. The experimental design is shown in Fig. 3D.

2.8. Enzyme-linked immunosorbent assay (ELISA)

Brain tissues and the conditioned medium (CM) of BV2 cells were collected for each group. The concentrations of HMGB1 and the cytokines IL-1β, IL-6 and TNF-α in the CM and brain tissues were detected by using an ELISA kit (SenBeiJia Biotechnology Co., Ltd., China). All of the steps of ELISA were performed according to the manufacturer's protocols.

2.9. Quantitative real-time polymerase chain reaction (qRT-PCR)

BV2 cells were washed 3 times with pre-cooled PBS after 0 h or 12 h of OGD/reperfusion (OGD/R), and the brain samples were lysed with Trizolreagent (Life Technologies, CA). Total RNA was extracted according to the manufacturer's protocol. The OD values and RNA concentration were determined by a spectrophotometer at 260 nm, and an OD value between 1.8 and 2.0 indicated that the sample could be used in the experiment. One microgram of RNA was reverse transcribed into 20 μl of cDNA using a commercial reverse transcription kit (Hiscript II Q RT SuperMix for qPCR; Vazyme, Nanjing, China) with a thermocycler according to the manufacturer's instructions. Two microliters of synthesized cDNA was subjected to qRT-PCR using specific primers and SYBR PCR Master Mix (Vazyme, Nanjing, China). The qRT-PCR protocol was as follows: an initial denaturation at 95 °C for 30 s followed by 40 cycles at 95 °C for 10 s and 60 °C for 30 s. At the end of the PCR, a melting curve was obtained by holding the samples at 95 °C for 15 s, cooling to 60 °C for 1 min, and then heating slowly at 0.3 °C/s until 95 °C was reached. This process was performed using a StepOnePlus™ real-time PCR machine. The primers are listed in Table 1. mRNA expression was normalized to the expression of the housekeeping gene β-actin using the $2^{-\Delta\Delta}$CT method.

2.10. Preparation of nuclear and cytoplasmic fractions

At the indicated time points, the treated BV2 cells were washed with pre-cooled PBS 3 times after the culture medium was removed, and the brain tissue samples were sonicated at a low temperature. Nuclear and cytoplasmic fractions were isolated using a cytoplasmic and nuclear protein extraction kit (KeyGEN Biotech, Nanjing, China) according to the manufacturer's instructions to determine HMGB1 translocation and nuclear NF-κB p65 content. Briefly, cytoplasmic proteins were extracted by using hypotonic lysis buffer (20 mM HEPES (pH 7.4), 2 mM EGTA, and 2 mM $MgCl_2$), and nuclear proteins were extracted by hypertonic

Table 1
List of primers used for qRT-PCR.

Gene	Species	Forward sequence (5′-3′)	Reverse sequence (5′-3′)
IL-1β	Mouse	TGTGTTTTCCTCCTTGCCTCTGAT	TGCTGCCTAATGTCCCCTTGAAT
IL-6	Mouse	TCACAGAAGGAGTGGCTAAGGACC	ACGCACTAGGTTTGCCGAGTAGAT
TNF-α	Mouse	GCTCTGTGAAGGGAATGGGTGT	CCAGGTCACTGTCCCAGCATCT
HMGB1	Mouse	GGAGTGGCTTTTGTCCCTCAT	TGCCTCTCGGCTTTTTAGGA
β-Actin	Mouse	GGGAAATCGTGCGTGAC	AGGCTGGAAAAGAGCCT

lysis buffer (20 mM Tris/HCl, pH 7.6, 100 mM NaCl, 20 mM KCl, 1.5 mM $MgCl_2$, and 0.5% Nonidet P-40 supplemented with phosphatase and protease inhibitors). The protein concentration of the lysates was determined *via* Western blotting by stripping the polyvinylidene difluoride (PVDF) membranes (Millipore, Billerica, MA, USA) and re-probing them with Lamin B1 (Proteintech Group, Rosemont, IL, USA) as a nuclear control and β-actin (Proteintech) as a cytoplasmic control.

2.11. Co-immunoprecipitation (co-IP)

BV2 cell lysates were prepared in IP lysis buffer (KeyGEN) supplemented with protease and phosphatase inhibitor cocktail on ice. Co-IP was performed to detect the acetylation level of HMGB1 and the interaction between HMGB1 and SIRT1. The procedure was performed according to the manufacturer's protocols. A total of 5 μg of a diluted rabbit polyclonal anti-HMGB1 antibody (Abcam) or a rabbit mAb IgG control (CST) was added to Protein A/G magnetic beads (MedChemExpress), and the Protein A/G magnetic bead-Ab complex was prepared by rotating at 4 °C for 2 h. Magnetic separation was performed on a magnetic stand, and after washing several times with a binding/wash buffer (1 × PBS + 0.5% Triton X-100, pH 7.4), the cell lysate antigen (Ag) was added to the complex. The protein A/G magnetic bead-Ab-Ag complex was produced by rotary incubation at 4 °C for 2 h. Magnetic separation was performed, and the supernatant was discarded. Then, 50 μl of 1 × SDS-PAGE loading buffer was added to the complex, and the complex was mixed uniformly and heated at 95 °C for 5 min. The magnetic beads were separated, and the supernatant was collected for SDS-PAGE detection.

2.12. Western blotting (WB)

After the brain tissues and cell lysates were prepared, the protein concentrations were determined with a Modified BCA Protein Assay Kit (KeyGEN), and the different samples were then adjusted to obtain equal concentrations. For WB, equal amounts of total or nuclear/cytoplasmic protein, along with 2 μl of molecular weight marker, were electrophoresed on SDS-PAGE gels. The gels were subjected to 150 V for 65 min. Next, the proteins were transferred to a PVDF membrane at 300 mA at a low temperature for 1–2 h. After non-specific sites were blocked with 5% non-fat dry milk or bovine serum albumin (BSA) in TBS containing 0.1% Tween-20 (TBST), the membranes were incubated with primary rabbit polyclonal anti-HMGB1 (1:1000), rabbit polyclonal anti-NF-κB p65 (1:1000, CST), mouse monoclonal anti-SIRT1 (1:1000, Proteintech), rabbit polyclonal anti-MyD88 (1:1000, CST), mouse monoclonal anti-TLR4 (1:1000, Proteintech), acetylated-lysine (1:1000, Abcam), mouse monoclonal anti-β-actin (1: 5000) and mouse monoclonal anti-Lamin B1 (1: 5000) antibodies at 4 °C overnight. β-Actin (for total protein and the cytoplasmic fraction) and Lamin B1 (for the nuclear fraction) were used as internal controls. After being washed with TBST three times, the membranes were incubated with the respective horseradish peroxidase-conjugated secondary antibody (1:10000, Yifeixue, BioTECH, Nanjing, China) at room temperature for 2 h. Immunoreactivity was visualized with the ECL Western Blotting Detection System (Millipore). Target proteins with molecular weight differences of < 5 kD from compared to the internal control were incubated antibody and visualized, and then the membrane was eluted with the antibody eluent, followed by incubation and visualization of the internal control. Grey value analysis was conducted with ImageJ software (National Institute of Health). The densities of specific bands were quantified and are expressed as a percentage of the β-actin or Lamin B1 band density.

2.13. Immunofluorescence

Twenty-four hours after HI insult, mouse brains were removed after cardiac perfusion with normal saline and 4% paraformaldehyde. The brain samples were fixed in 4% paraformaldehyde for 24 h and then dehydrated in a 20–30% sucrose solution gradient. Subsequently, brain samples embedded in OCT freezing medium (Sakura) were cut into 20-μm cryosections using a freezing microtome (ThermoFisher Scientific). The cryosections were incubated with mouse anti-Iba1 (1:500, Wako Chemicals, Japan) and rabbit anti-HMGB1 (1:500, Abcam) overnight at 4 °C followed by incubation with Alexa Fluor 488- or 552-conjugated goat anti-rabbit or Alexa Fluor 552-conjugated anti-mouse secondary antibodies (1:200, Beyotime Biotechnology) for 1 h at room temperature in the dark. Nuclei were counterstained with DAPI (1:2000, KeyGENE). Fluorescent confocal images were captured with an FV10-ASW 3.1 Viewer on a confocal laser scanning microscope (Olympus, FV1000, Japan).

BV2 cells or primary neurons were fixed in 4% paraformaldehyde for 15 min and permeabilized in 0.2% Triton X-100/PBS, followed by blocking for 1 h with BSA at room temperature. Then, primary neurons were incubated with mouse anti-HMGB1 (1:500, Proteintech) and rabbit anti-NeuN (1:500, CST). Meanwhile, BV2 cells were incubated with rabbit anti-HMGB1 overnight at 4 °C and then incubated with a secondary antibody for 1 h at room temperature in the dark. Nuclei were counterstained with DAPI. Immunofluorescence intensity was quantified using ipwn32 software by measuring the staining intensity in six different fields. For the quantitative analysis of HMGB1 translocation, cells with diffuse HMGB1 in the cytoplasm were defined as translocation-positive.

2.14. SIRT1 activity assay

To assay cellular SIRT1 activity, proteins were extracted from BV2 cells after exposure to the different treatments described above. A SIRT1 Fluorometric Assay Kit (Sigma, CS1040) was used to quantify SIRT1 activity according to the manufacturer's protocol. Fluorescence intensities were measured with a microplate fluorometer (excitation wavelength, 360 nm; emission wavelength, 450 nm).

2.15. Lactate dehydrogenase (LDH) release assay

The release of LDH from damaged cells into the culture medium is a marker of cell damage. To evaluate LDH release, primary neurons were seeded in 96-well plates at a density of 2×10^4 cells/well, and the supernatant was collected after the addition of BV2 cell CM for 24 h. LDH release was measured by an LDH Cytotoxicity Assay Kit (Beyotime) according to the manufacturer's instructions. The optical densities were determined by measuring the absorbance at 490 nm using a microplate reader. The results were calculated by the following formula: LDH cytotoxicity (%) = $(OD_{treated} - OD_{blank})/(OD_{maximum\ cell\ enzyme\ activity} - \text{sample } OD_{reference}) \times 100$.

2.16. Statistical analysis

The results are expressed as the mean ± standard deviation (SD) and were analysed by SPSS 22.0 software (SPSS, Chicago, IL, USA). For comparisons of the differences between the two groups, the data were statistically assessed by Student's *t*-test (two-tailed), while multiple group analysis was performed using one-way analysis of variance (ANOVA) followed by Bonferroni multiple comparisons test. All experiments were performed at least in triplicate. Differences were considered significant at $p < 0.05$.

3. Results

3.1. RES attenuates HI insult-induced brain damage and neurobehavioral defects

HI led to obvious brain damage, and histological examination showed disruption of hippocampal and cortical morphology and

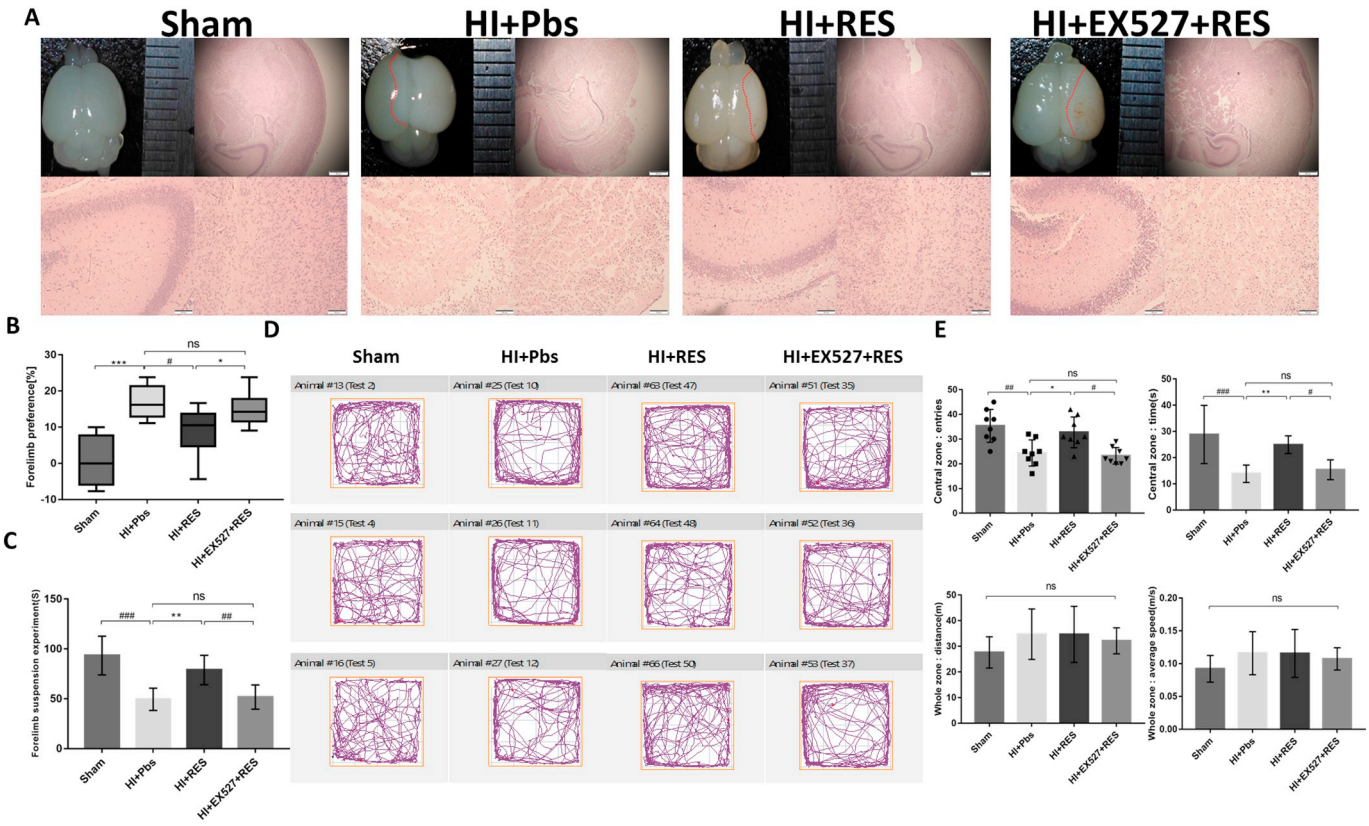

Fig. 1. Effects of Resveratrol on brain damage and behavioural performance.
(A) Effects of resveratrol on brain damage. Representative images of whole-brain and HE staining in the cortex and hippocampus 24 h after HI insult are shown (the right side of the dotted red line indicates the area of brain damage) (HE, 40× and 200×). (B, C) The asymmetry of forelimb use was evaluated by the cylinder test (B), and muscle strength was evaluated by a forelimb suspension experiment (C). (D, E) Representative behavioural tracks of the experimental mice and the statistical results of different indicators in the open-field test. n = 12 in each group for the HIBI model and 8 for the behavioural tests. Statistical significance was determined by one-way ANOVA followed by Bonferroni multiple comparisons test. The values are expressed as the mean ± standard deviation: ns, $p > 0.05$; *, $^{\#}$, $p < 0.05$; **, $^{\#\#}$, $p < 0.01$; ***, $^{\#\#\#}$, $p < 0.001$. (For interpretation of the references to colour in this figure legend, the reader is referred to the web version of this article.)

massive immune cell infiltration (Fig. 1A). Meanwhile, behavioural tests revealed that the number of entries into and the time spent in the central zone but not the distance travelled throughout the entire open-field arena or the average speed in the open-field test were decreased (Fig. 1D, E); additionally, muscle strength (Fig. 1C) and the symmetry of limb activity (Fig. 1B) were impaired. These abnormalities were significantly ameliorated after RES administration. To determine whether SIRT1 is involved in the neuroprotective effect of RES in this HIBI model, a specific inhibitor of SIRT1, EX527, was injected prior to RES administration. We found that EX527 significantly reversed the neuroprotective effects of RES.

3.2. RES suppresses neuroinflammatory responses by inhibiting the TLR4/MyD88/NF-κB signalling pathway in vivo

We investigated whether RES improves HI insult-induced brain damage and behavioural defects in experimental animals by affecting the neuroinflammatory responses. The results showed that the mRNA and protein levels of the cytokines IL-1β, IL-6, and TNF-α in brain tissues after HI insult were significantly elevated, but resveratrol reduced this abnormal increase (Fig. 2A, B). Therefore, we asked which potential signalling pathway regulated by RES is responsible for this phenomenon. The WB results indicated that HI-induced decreased levels of SIRT1, as well as elevated levels of TLR4, MyD88, and nuclear NF-κB, were reversed by resveratrol, whereas the administration of EX527, compared with HI + RES, partially abolished this anti-neuroinflammatory effect (Fig. 2C, D).

3.3. HMGB1 cytoplasmic localization in microglia increases after HI insult and can be diminished by RES

Since SIRT1 is indeed involved in the inhibition of TLR4 signalling by resveratrol, we hypothesized that HMGB1 acts as a link between these two molecules; interestingly, however, there was no significant difference in HMGB1 mRNA levels between the sham group and the HI + PBS group or the other drug-administered groups (Fig. 2E). According to the viewpoint that the function of HMGB1 is mainly related to its localization in cells and microglia plays a key role in the occurrence and development of neuroinflammation after HI insult [10], we speculated that the changes in the localization of HMGB1 were involved in this inflammatory process.

To explore the relationship between microglia and HMGB1 *in vivo* and determine whether HMGB1 is involved in microglial-mediated neuroinflammation after HI insult, we focused on the distribution of HMGB1 in microglia. Confocal imaging using antibodies against HMGB1 and the microglia cell-specific marker Iba1 showed that the expression of Iba1 was weak and that HMGB1 was located in the nucleus of the microglia in the sham group. After HI insult, the fluorescence intensity of Iba1 dramatically surged, and HMGB1 was partially localized outside the nucleus, implying that the activation of microglia was accompanied by increased nucleoplasmic transfer of HMGB1. RES had the ability to attenuate the increased expression of Iba1 induced by HI insult and reduce the cytoplasmic localization of HMGB1. Meanwhile, the HI + EX527 + RES group showed a dramatic increase in the extracellular and cytoplasmic distribution of HMGB1. A representative confocal image is shown in Fig. 2E.

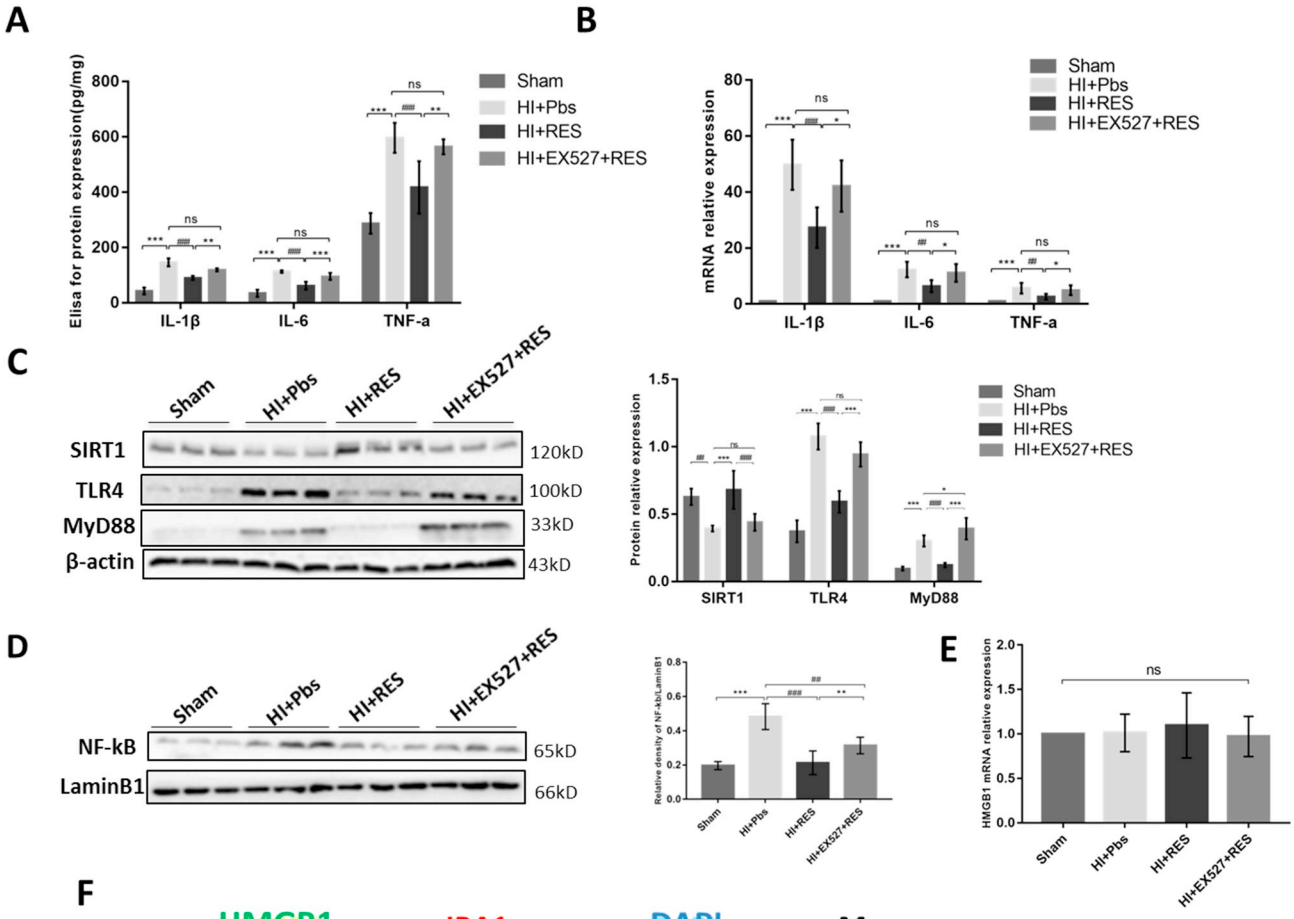

(caption on next page)

Fig. 2. Effects of resveratrol on the TLR4 signalling pathway, cytokine expression and microglial HMGB1 release *in vivo*.
(A, B) The protein and mRNA expression of IL-1β, IL-6 and TNF-α were determined by ELISA and qRT-PCR, respectively. (C, D) Total protein and nuclear protein extracted from brain tissues were analysed for protein levels of SIRT1, TLR4, MyD88 and nuclear NF-κB and Lamin B1 by Western blotting. Representative western bands and the quantification are shown. (E) The mRNA expression of HMGB1 was determined by qRT-PCR. (F) Representative confocal images of Iba1 expression and HMGB1 localization in microglia in the lesioned cortices. Double staining was used to assess microglial activation and HMGB1 translocation in the lesioned cortex 24 h after HI insult. Compared with that in the sham group, the fluorescence intensity of Iba1 and cytoplasmic HMGB1 staining increased after HI insult. The HI + RES group exhibited weak Iba1 fluorescence intensity and less HMGB1 cytoplasmic localization. n = 4–6 in each group for confocal immunofluorescence microscopy; n = 6 for the other tests. Statistical significance was determined by one-way ANOVA followed by Bonferroni multiple comparisons test. The values are expressed as the mean ± standard deviation: ns, $p > 0.05$; *, #, $p < 0.05$; **, ##, $p < 0.01$; ***, ###, $p < 0.001$. Scale bar, 10 μm.

3.4. RES mitigates inflammation of BV2 cells after OGD by inhibiting TLR4 signalling in vitro

We found in the *in vivo* experiment that HI led to the activation of microglia and increased the extracellular and cytoplasmic localization of HMGB1 and the activation of the signalling pathways mediated by the HMGB1 reciprocal receptor TLR4. In addition, RES and EX527 attenuated and aggravated this change, respectively. To further explore the mechanism of this phenomenon, mouse microglial BV2 cells were selected for *in vitro* experiments. First, the optimal experimental drug concentrations of RES or EX527 were determined to be 25 μM and 100 μM, respectively, by the CCK-8 assay (Fig. 3A, B), and no significant effect on cell viability was observed upon OGD treatment for 3 h (Fig. 3C).

In subsequent experiments, it was found that, compared with that in the control group, OGD significantly increased the mRNA expression of IL-1β, IL-6 and TNF-a in BV2 cells (Fig. 3E), the protein levels of the above three cytokines in the CM (Fig. 3F), and the expression of TLR4, MyD88, and nuclear NF-κB (Fig. 3G, H); pretreatment with RES inhibited this amplification of inflammation. However, the administration of EX527 restored the cytokine protein expression to the level observed in the OGD + DMSO group, but this effect was not observed at the mRNA level.

3.5. RES inhibits OGD-induced HMGB1 release in BV2 cells by activating SIRT1 to reduce the acetylation of HMGB1

We speculated that the aforementioned experimental phenomenon may be involved in the changes in HMGB1 caused by RES intervention. To validate our hypothesis, we directly examined the changes in HMGB1 in BV2 cells after OGD. Confocal imaging and quantitative results showed that, compared with that in the control group, HMGB1 localization in the cytoplasm was enhanced significantly after OGD (Fig. 4A, B), and HMGB1 content in the CM was dramatically increased (Fig. 4C). In addition, nuclear-cytoplasmic separation also revealed that HMGB1 was transferred from the nucleus to the cytoplasm (Fig. 4E), demonstrating that BV2 cells released HMGB1 after OGD. RES altered this release, and this was manifested as increased HMGB1 retention in the nucleus; conversely, pretreatment with EX527 exacerbated this phenomenon. Interestingly, however, there was no significant difference in the mRNA levels of HMGB1 among the groups immediately after OGD or 12 h after OGD/R (Fig. 4D), again proving that the increase in the extracellular HMGB1 level was mainly due to enhanced active release by BV2.

Because acetylation plays an important role in the active release of HMGB1 and because SIRT1 activators and inhibitors can attenuate or enhance this type of HMGB1 release after OGD, we further investigated whether SIRT1 can directly participate in the acetylation of microglial HMGB1 during OGD. To confirm that SIRT1 indeed directly interacts with HMGB1 and participates in its nucleocytoplasmic translocation and release, we performed a co-IP experiment after OGD and discovered that SIRT1 expression was decreased, acetylated HMGB1 levels were elevated, and the interaction between HMGB1 and SIRT1 was diminished (Fig. 4F, G). RES increased the interaction between SIRT1 and HMGB1 by increasing the expression and deacetylase activity of SIRT1, thereby reducing the level of HMGB1 acetylation and ultimately inhibiting HMGB1 nucleocytoplasmic translocation. Although EX527 had no substantial effect on SIRT1 expression after OGD, it augmented the active secretion of HMGB1 by inhibiting the deacetylase activity of SIRT1 (Fig. 4G, H).

3.6. Effects of BV2 cell CM from different treatment groups on primary neurons

Finally, as the inflammatory cascade can cause secondary damage to neurons, we researched the effect of BV2 cells from different treatment groups on primary neurons. The CM from BV2 cells from each treatment group was collected after OGD/R and added to primary neurons for co-culture. After 24 h, an evaluation of LDH release revealed that the CM from the OGD group caused neuronal damage, while that from the OGD + RES group showed a certain protective effect. Additionally, confocal imaging using antibodies against HMGB1 and the neuron cell-specific marker anti-NeuN showed that the CM from the OGD group led to pronounced extracellular localization of HMGB1 in neurons, but RES inhibited this translocation (Fig. 5).

4. Discussion

RES is considered to be a potential drug for the treatment of neurological diseases, including ischemic brain disease, and it reduces the extent of brain damage when administered before or after ischemia in rodent models. The neuroprotective mechanisms of RES might include antioxidation, anti-inflammation, and antiapoptosis effects. Recent studies have reported that RES suppresses the inflammatory response by inhibiting TLR4 signal transduction in several disease models [32–35].

HMGB1 can be post-transcriptionally modified, primarily by the acetylation of lysine at two nuclear localization sites, to affect its localization in the cells [36]. Hyperacetylation-mediated HMGB1 nucleoplasmic transfer and the active release of HMGB1 occurs after immune cells are stimulated [37]. Actively released HMGB1 is able to in turn stimulate the host cell itself and adjacent cells, playing autocrine and paracrine role and thus leading to the amplification of inflammation and the maintenance of damage caused by inflammation [38]. Although there have been many studies on the effects of HMGB1 on brain injury in adult rodents, at present, information regarding the effect of HI insult on the dynamics of HMGB1 in the perinatal brain is very limited. A clinical study reported that umbilical arterial HMGB1 levels are elevated in HIE infants compared with controls and decrease after brain hypothermic therapy, indicating that neuroinflammation that involves HMGB1 may play a role in the neuroprotective mechanism of hypothermic therapy [25]. In addition, HMGB1 serum levels were confirmed to be elevated in neonates with asphyxia-related brain injury within 30 min after birth, suggesting that HMGB1 can be used as an early biomarker for brain damage caused by perinatal asphyxia [39]. A recent study on neonatal rat HIBI demonstrated time-dependent HMGB1 translocation, but it did not explore the mechanism by which HMGB1 triggers downstream inflammation [40].

Microglia play a predominant role in the development of neuroinflammation in HI insult-induced acute brain injury and damage neighbouring cells through chronic overstimulation and a prolonged inflammatory response. We found that microglial cells exhibited

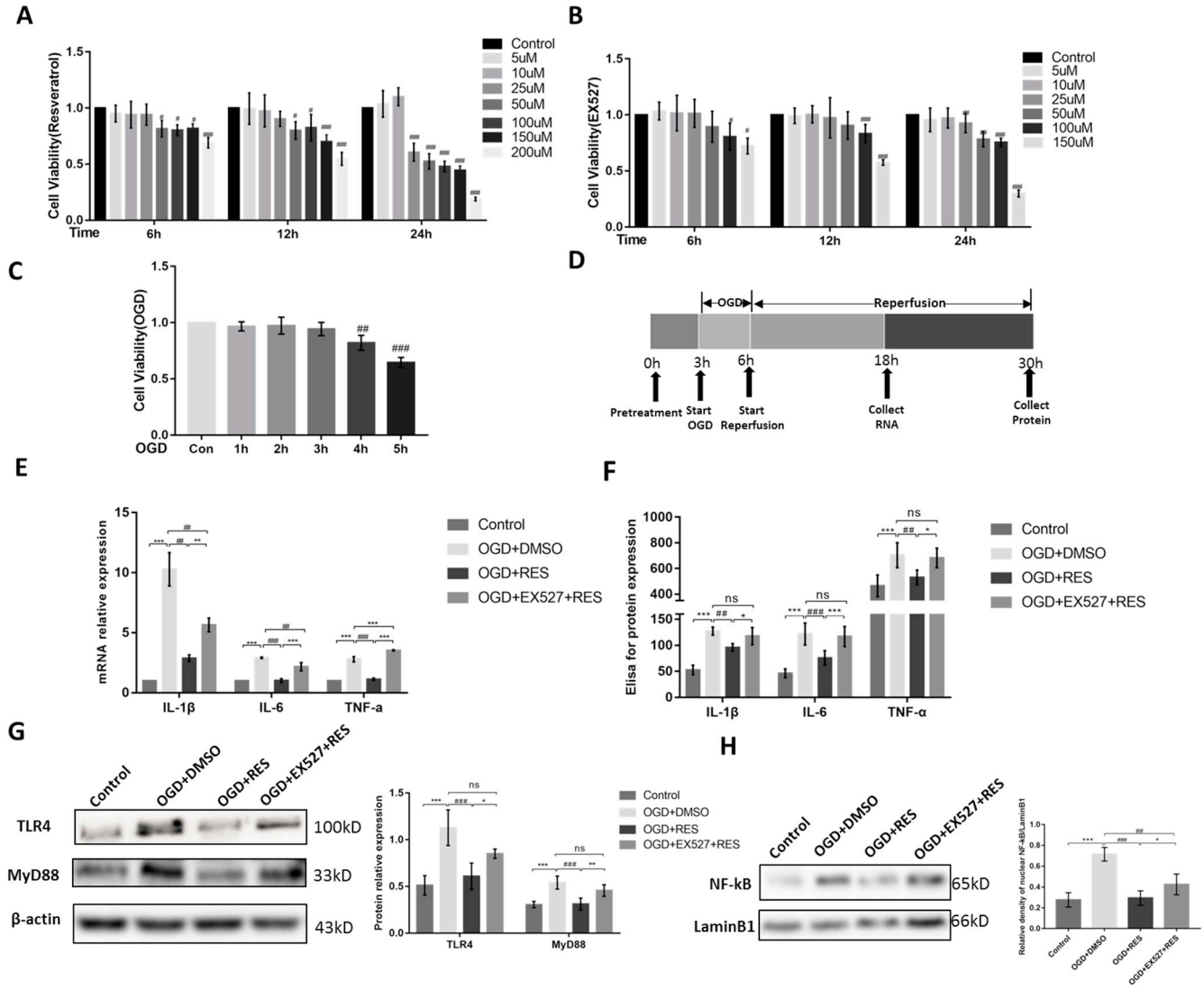

Fig. 3. Cell viability of BV2 microglial cells exposed to different treatments, as determined by the CCK-8 assay, and the effects of resveratrol on the TLR4 signalling pathway and cytokine expression *in vitro*.

(A, B) BV2 cells were incubated with resveratrol or EX527 (0, 5, 10, 25, 50, 100, 150 and 200 μM) for 6 h, 12 h or 24 h. (C) BV2 cells were subjected to oxygen glucose deprivation for 1 h, 2 h, 3 h, 4 h or 5 h. (D) A schematic diagram of the *in vitro* experiment. (E, F) The mRNA and protein expression of IL-1β, IL-6 and TNF-α in the condition medium was determined by qRT-PCR and ELISA, respectively. (G, H) The protein levels of TLR4, MyD88, nuclear NF-κB and Lamin B1 in BV2 cells were determined by Western blotting. Representative western bands and the quantification are shown. Statistical significance was determined by Student's *t*-test (two-tailed) or one-way ANOVA followed by Bonferroni multiple comparisons test. The values are expressed as the mean ± standard deviation: ns, $p > 0.05$; *, $^{\#}$, $p < 0.05$; **, $^{\#\#}$, $p < 0.01$; ***, $^{\#\#\#}$, $p < 0.001$. n = 4 replicates for each test.

obvious HMGB1 nucleocytoplasmic translocation after HI insult, which is in conflict with the results of Chen et al., who did not detect HMGB1 translocation in microglia after HI [40]. They asserted that microglia have relatively small cell bodies with small cytosolic compartments, which might render it more challenging to detect an apparent shift in HMGB1 from the nucleus to the cytosol. We do not endorse this explanation because microglia undergoes a series of morphological changes, such as an enlargement of the cell body, which is beneficial for observation, after experiencing stress. In addition, in our *in vivo* studies, we used a 1000× oil lens for confocal imaging to clearly observe the cytoplasmic localization of HMGB1 in microglia 24 h after HI insult, and similar findings were obtained in our *in vitro* studies. Frasch et al. [41] used umbilical cord occlusion to mimic hypoxic acidemia that might occur during labour and demonstrated that HMGB1, which is normally located in the nucleus of α7nAChR-containing microglia from ovine foetuses, underwent nucleocytoplasmic translocation after injury; this further confirmed the shift of HMGB1 from the nucleus to the cytoplasm in microglia after HI insult. In the *in vitro* experiments, the HMGB1 protein level was almost identical before and after OGD, presumably because the release of the nucleus of HMGB1 was not sufficient to cause changes in the overall protein level, and the lack of a change in HMGB1 mRNA expression upon treatment with OGD was not able to change the protein expression.

Our study is the first to provide evidence that HMGB1 and TLR4 are potentially involved in the neuroprotective effects of RES on neonatal HIBI. A recent report demonstrated that TLR4 plays a role in HI insult -induced brain injury [42], the focus of this study was on the role of the HMGB1-TLR4 axis in the anti-neuroinflammatory effects of RES. Although RES had no significant effect on the expression level of HMGB1 after OGD, it was able to influence the downstream TLR4 inflammatory signalling pathway by regulating HMGB1 release. Both *in vivo* and *in vitro*, we found that HI insult- and OGD-induced inflammation was partially associated with a significant increase in TLR4 and MyD88 expression and accompanied by increased nuclear NF-κB levels, which

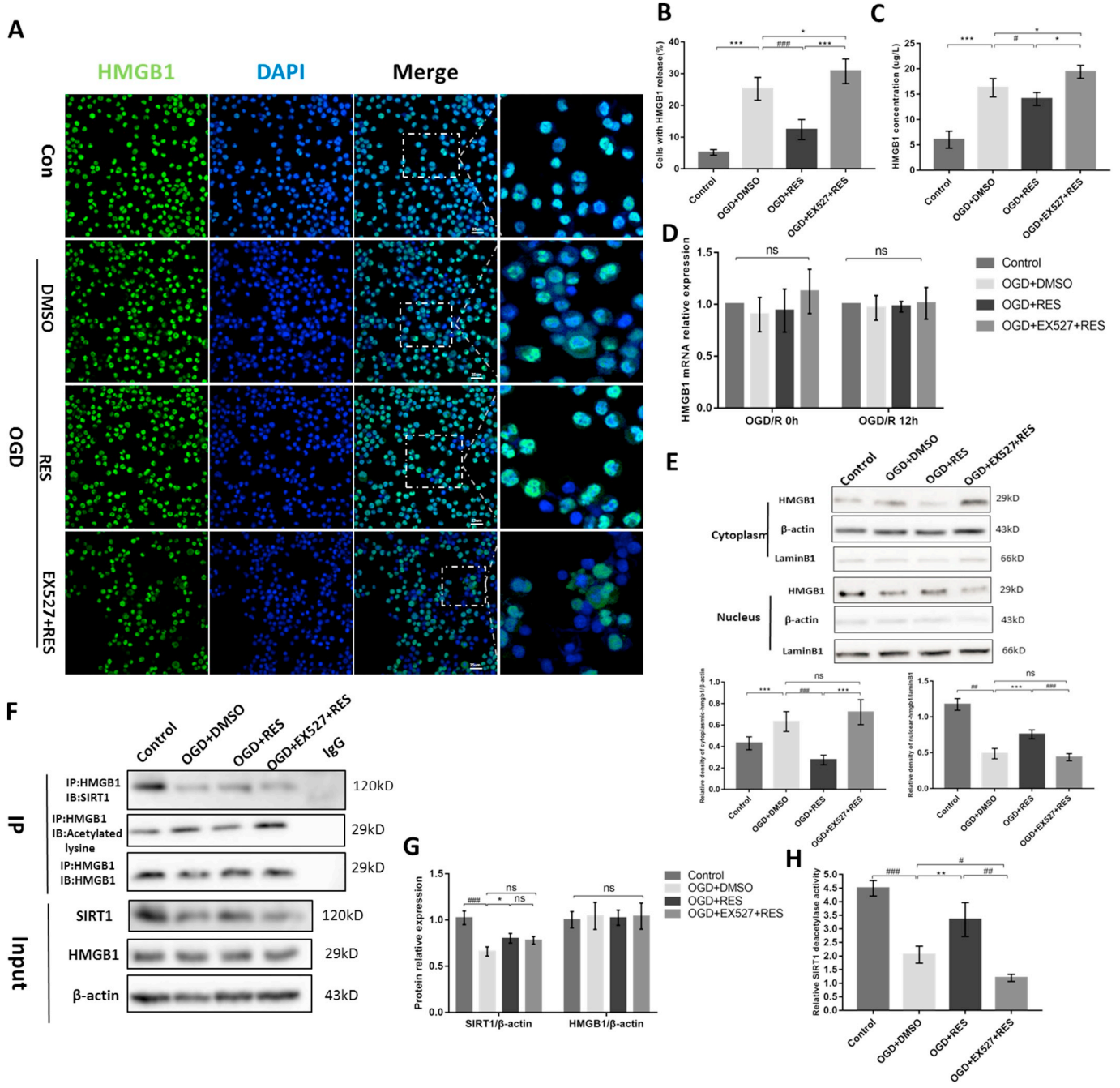

Fig. 4. Resveratrol participates in the acetylation of HMGB1 through SIRT1.
(A, B) Representative confocal images of HMGB1 localization in BV2 cells. HMGB1 was stained green, and the nuclei were stained blue with DAPI. (C) The concentration of HMGB1 in BV2 conditioned medium was measured by ELISA. (D) The qRT-PCR results showed no significant difference in the mRNA expression of HMGB1 0 h or 12 h after OGD. (E) The protein expression of HMGB1 in the nuclear and cytoplasmic fractions was determined by Western blotting. Representative western bands and the quantification are shown. (F, G) Co-IP and Western blotting were used to determine the direct interaction between HMGB1 and SIRT1. Representative western bands and the quantification are shown. (H) The relative deacetylase activity of SIRT1 in each experimental group was determined. n = 6 replicates for confocal immunofluorescence microscopy and ELISA; n = 4 replicates for qRT-PCR and Western blot. Statistical significance was determined by one-way ANOVA followed by Bonferroni multiple comparisons test. The values are expressed as the mean ± standard deviation: ns, $p > 0.05$; *, #, $p < 0.05$; **, ##, $p < 0.01$; ***, ###, $p < 0.001$. Scale bar, 25 μm. (For interpretation of the references to colour in this figure legend, the reader is referred to the web version of this article.)

is consistent with previous reports [43,44]. TLR4 is mainly expressed in microglia in the central nervous system [45], and it is known to induce microglial pro-inflammatory responses to many stimuli. Since microglial activation is extensively controlled by pathogen recognition receptors, TLR4 is involved in the microglia-mediated neurotoxicity that occurs in many brain pathologies. If the TLR4 pathway is erroneously activated or if the signal is uncontrollably amplified, the cytokine response may have a detrimental effect on the nervous system. TLR4 signalling exacerbates stroke outcomes, including the infarct volume, neurological function, and inflammatory markers [46], while TLR4-deficient mice show improved neurological and/or behavioural outcomes in various models of cerebral infarction [47]. In general, TLR4-mediated inflammatory signalling has the ability to guide necrosis and apoptosis in various cell types in the central nervous system [48]. Other

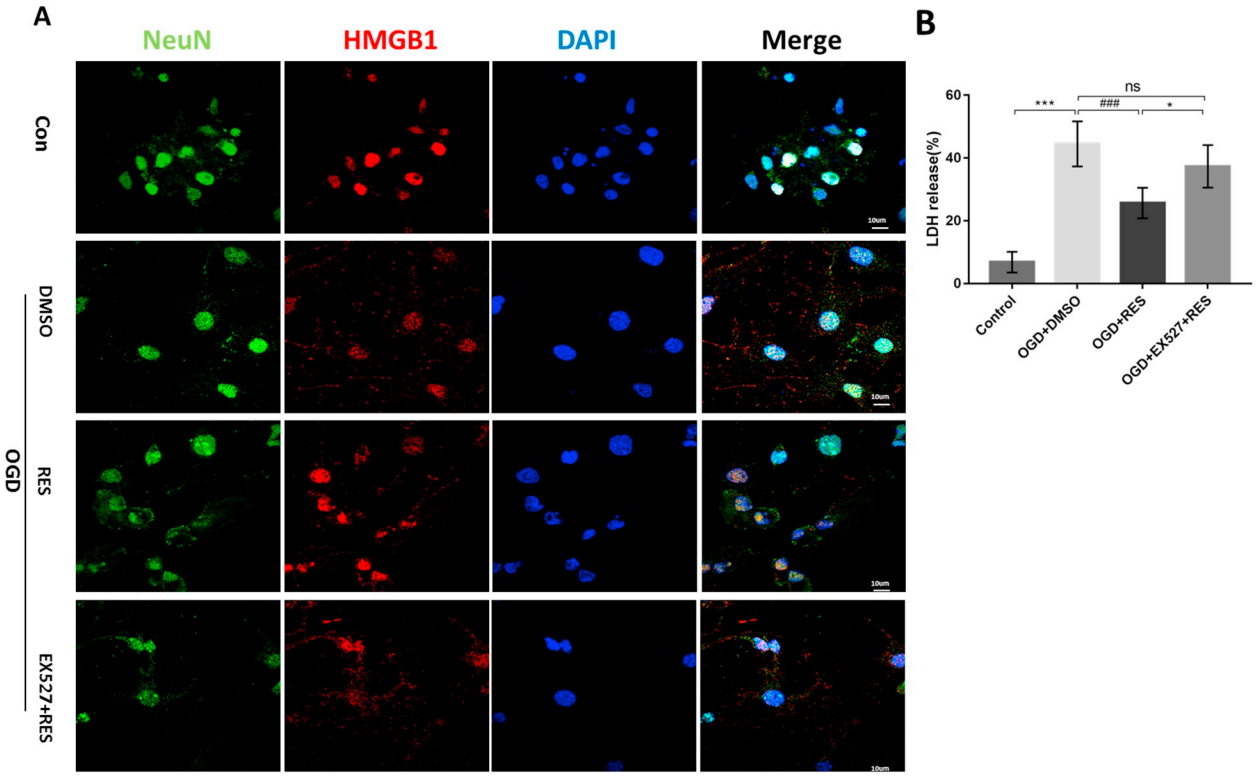

Fig. 5. Effect of BV2 conditioned medium on primary neurons.
(A) Representative confocal images of the co-localization of primary neurons (NeuN, green) with HMGB1 (red) following the addition of conditioned medium from treated BV2 cells. (B) LDH release from the supernatant of primary neurons from each group was determined. n = 4 replicates. Statistical significance was determined by one-way ANOVA followed by Bonferroni multiple comparisons test. The values are expressed as the mean ± standard deviation: ns, $p > 0.05$; *, $p < 0.05$; ***, $^{###}$, $p < 0.001$. Scale bar, 10 μm. (For interpretation of the references to colour in this figure legend, the reader is referred to the web version of this article.)

molecules, such as HIF-1α, SOCS-1, and PCG-1α, also play an important role in the neuroinflammatory response mediated by microglia activation. The effects of RES may be mediated by these molecules [49,50], but in our study, we focused on the role of HMGB1 in HI insult-induced neuroinflammation and attempted to elucidate the new mechanism by which RES provides neuroprotection; thus, we focused on TLR4, the classical receptor of HMGB1. Whether RAGE and other TLRs (also known as HMGB1 receptors) are altered after HI insult and whether RES can regulate them will be further studied.

The results demonstrated that RES activated SIRT1 to deacetylate HMGB1 and thus attenuate its translocation, which may have inhibited the inflammatory response mediated by the downstream TLR4 signalling pathway. As a vital deacetylase, SIRT1 plays an important role in the regulation of cellular metabolism, autophagy and chromatin accessibility and is associated with a variety of pathophysiological processes. It has been reported that SIRT1 expression is decreased in neonatal HIBI [51], and RES, as the most efficacious SIRT1 activator [52], can increase the activity of human SIRT1 by as much as eight-fold by reducing the *K*m value of the acetylated substrate [52,53]. RES can inhibit microglial activation and the inflammatory response after HI insult [17] and thus downregulate the TLR4 signalling pathway to mitigate brain damage in a focal cerebral ischemia model in adult rats [32]. Our results revealed that RES does not affect HMGB1 expression *in vivo* and *in vitro* but inhibits its acetylation level and release. Other studies have confirmed that some pharmaceuticals inhibit the HMGB1/TLR4/NF-κB signalling pathway by activating SIRT1 [54]. Therefore, we confirmed that the anti-inflammatory effect of RES is partly achieved by interfering with TLR4 signal transduction *via* activating SIRT1 to regulate the release of HMGB1.

Unexpectedly, although more HMGB1 release was observed in the group treated with EX527 (a SIRT1 inhibitor), EX527 did not appear to cause a more serious inflammatory response or simultaneous brain damage. We believe that this is related to the pharmacological mechanism of EX527 or another pathophysiological mechanism. Beier et al. reported that SIRT1 deletion or pharmacological inhibition by EX527 leads to an increase in SIRT1-mediated Foxp3 mRNA expression and thereby suppresses the immune response [55]. In a study that investigated the use of placenta-derived mesenchymal stem cell (PD-MSC) transplantation to treat neonatal rat HIBI, the researchers found that the number of Tregs in the spleens of the HIBI group increased dramatically and that PD-MSCs repressed the neuroinflammatory response after HIBI by increasing the number of Tregs and Foxp3 expression levels [56]. In addition, EX527 also has a protective effect on cerebral ischaemia reperfusion injury in adult rats through attenuating the necroptosis signalling pathway [57]. The precise mechanism underlying the effect of EX527 in HIBI requires more in-depth research, and the use of SIRT1 interference technology may be a better alternative.

Regarding the influence on neurons by interventions that affect microglial HMGB1 release, our results showed that, after co-culturing primary neurons with microglia CM, damage to the neurons was accompanied by the release of HMGB1, which suggests that HMGB1 can be used as a biomarker of injury. Since RES can directly alleviate neuronal damage caused by OGD/R [58,59], in order to distinguish this effect, this study did not directly detect neuronal damage in *in vivo* experiments or treat primary neurons with OGD or RES; instead, CM from microglia exposed to different treatment was collected to treat neurons *in vitro*. Since inflammatory factors contained in CM can directly cause neuronal damage [60], the degree of damage exhibited by the neurons from different treatment groups may be related to the differences in inflammatory factor levels in the microglia, which further confirms that resveratrol exerts neuroprotective effects by inhibiting the inflammatory response of microglia. As expected, the lower levels of

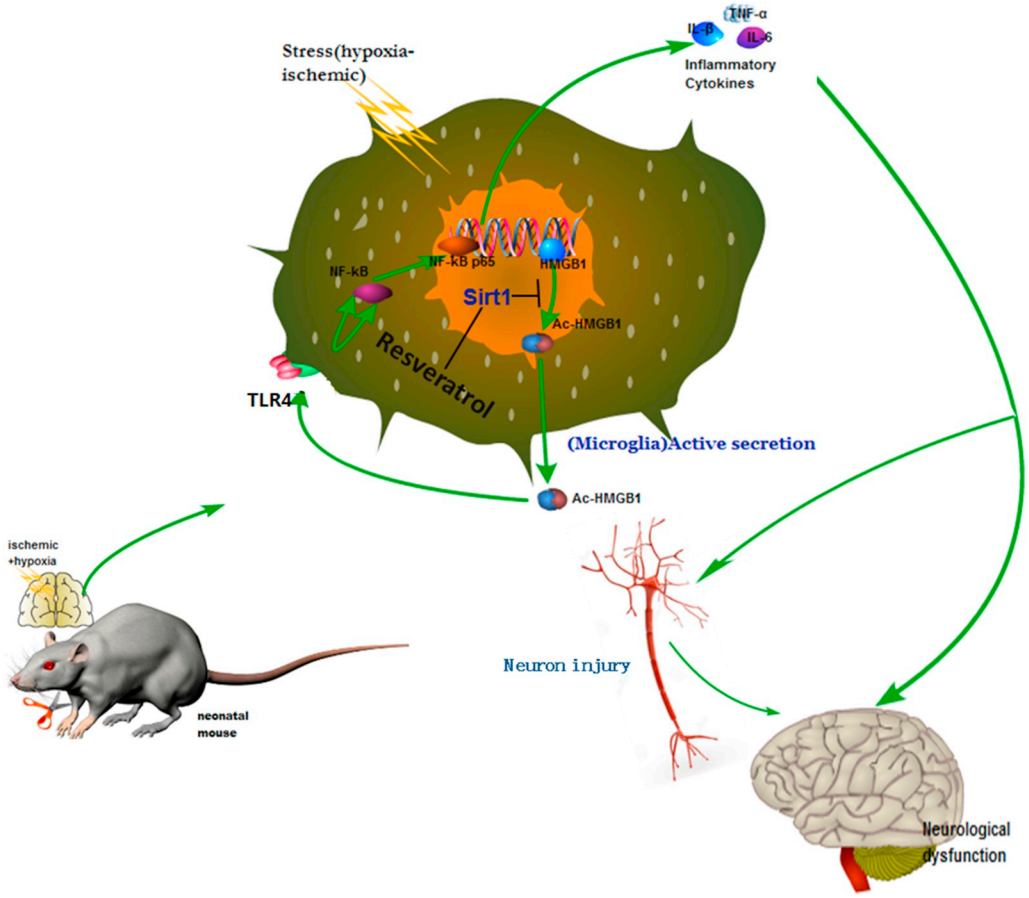

Fig. 6. Schematic illustration of the anti-neuroinflammatory mechanism of resveratrol in hypoxic-ischaemic brain injury involving the regulation of HMGB1 release by activated microglial SIRT1.
As illustrated, HI insult-induced reactive microglia actively release acetylated HMGB1 (Ac-HMGB1), which in turn activates the TLR4/MyD88/NF-kB signalling pathway in microglia to initiate a glial-neuronal neuroinflammatory response by producing a wide array of pro-inflammatory factors and mediators such as IL-1β, IL-6 and TNF-α. Resveratrol inhibits the acetylation of HMGB1 by activating SIRT1, thereby preventing the activation of the TLR4 signalling pathway by extracellular HMGB1.

damage observed in the RES group may be associated with a reduction in the inflammatory response, which is consistent with the results of Zhang et al. [61].

The significance of our research is that there are differences in immune mechanisms between neonatal HIE and adult ischemic stroke and that HMGB1 dynamics are different after damage to mature and immature brains. Considering that research over the past two decades has focused on the roles of HMGB1 in the extracellular space in inflammation, some people have suggested treating diseases by inhibiting or deleting HMGB1, but it is worth remembering that HMGB1 is also essential for life and for tissue regeneration processes. As an intrinsic non-histone nuclear protein, HMGB1 itself participates in many normal physiological processes. Thus, the study by Choi et al. should serve as an important guide because they alleged that the administration of the HMGB1-specific inhibitor glycyrrhizin into the internal capsule aggravates oligodendrocyte death, enhances demyelination and exacerbates sensorimotor behavioural deficits by inhibiting the autocrine trophic factor HMGB1 in a murine stroke model [62]. Oligodendrocyte injury and myelination disorders are thought to play an important roles in the sequelae of hypoxic-ischemic injury in immature brains [63]. In addition, a lack of HMGB1 does not disrupt cell growth but causes lethal hypoglycaemia in newborn mice [64], and astrocytic HMGB1 promotes endothelial progenitor cell-mediated neurovascular remodelling during stroke recovery [65]. From a therapeutic point of view, silencing HMGB1, although technically achievable, could be precarious, especially for neonates whose nervous system is still in the developmental stage, as it may deprive the host cells of the number of nuclear housekeeping functions of this molecule. Conversely, it seems to be more rational to attempt to correct the intracellular distribution of HMGB1 through SIRT1 activation and improve nuclear retention during stress. There are currently no specific treatments for neonatal HIE, and it is imperative to identify a technique that can specifically inhibit the secretion of HMGB1 in microglia. Therefore, RES, which inhibits the release of HMGB1 by reducing the level of HMGB1 acetylation *via* activating SIRT1, may be a potential drug for disease management.

We acknowledge that, although the present study provides an evaluation of the mechanisms by which RES inhibits the HMGB1-TLR4 axis to alleviate neonatal HIBI by SIRT1 *in vitro* and *in vitro*, there are important limitations that provide opportunities for further study. The effects of RES on SIRT1 are very extensive and difficult to predict accurately. SIRT1 is able to promote pro-inflammatory factor transcription through the acetylation of NF-κB at lysine K310, but we partially distinguished this effect by studying TLR4, the reciprocal receptor of HMGB1, and downstream MyD88. Such a distinction is an important area for further study, especially when neuroprotective strategies are being considered. A growing body of evidence has validated that increased HMGB1 levels are capable of inducing the upregulation of TLR4 [66]. Since one of the goals of our experiments was to illustrate the direct interaction between SIRT1 and HMGB1, the results we obtained are sufficient to demonstrate this. Another consideration is that neurons and other nerve cells can also release HMGB1 in a passive manner during necrosis after HI injury; determining the importance of HMGB1 in different cells during the inflammatory response after HI injury requires more advanced methods. Finally, extracellular HMGB1 can also stimulate the inflammatory response by binding with other receptors, such as RAGE and TLR2, and whether these related receptors are also involved in the anti-neuroinflammatory effects of RES on SIRT/HMGB1 requires further study.

5. Conclusions

In conclusion, microglia can actively release HMGB1, which enhances inflammatory factor expression by activating the HMGB1/TLR4/MyD88/NF-κB signalling pathway, in neonatal HIBI to

participate in neuroinflammation. RES treatment increases the direct interaction between SIRT1 and HMGB1 by increasing the expression and activity of SIRT1 and then reduces the acetylation of HMGB1, inhibits the nucleocytoplasmic translocation and subsequent release of HMGB1 from microglial cells, ultimately attenuates the downstream inflammatory cascade induced by this molecule, and improves brain damage and behavioural impairment caused by HI insult (Fig. 6). The anti-neuroinflammatory effects induced by limiting the translocation of HMGB1 to the nucleus provides new and complementary insights into the neuroprotective effects of RES and affords a new direction for the treatment of neonatal HIE.

Declaration of Competing Interest

The authors declare that they have no competing interests.

Acknowledgement

This study was supported by the National Natural Science Foundation of China (NO. 81471187).

Availability of data and materials

The datasets used and/or analysed in the current study are available from the corresponding author on reasonable request.

References

[1] S. Shankaran, Hypoxic-ischemic encephalopathy and novel strategies for neuroprotection, Clin. Perinatol. 39 (4) (2012) 919–929.
[2] P.D. Gluckman, J.S. Wyatt, D. Azzopardi, R. Ballard, A.D. Edwards, D.M. Ferriero, R.A. Polin, C.M. Robertson, M. Thoresen, A. Whitelaw, A.J. Gunn, Selective head cooling with mild systemic hypothermia after neonatal encephalopathy: multicentre randomised trial, Lancet 365 (9460) (2005) 663–670.
[3] D. Azzopardi, B. Strohm, N. Marlow, P. Brocklehurst, A. Deierl, O. Eddama, J. Goodwin, H.L. Halliday, E. Juszczak, O. Kapellou, M. Levene, L. Linsell, O. Omar, M. Thoresen, N. Tusor, A. Whitelaw, A.D. Edwards, T.S. Group, Effects of hypothermia for perinatal asphyxia on childhood outcomes, N. Engl. J. Med. 371 (2) (2014) 140–149.
[4] S. Shankaran, A. Pappas, S.A. McDonald, B.R. Vohr, S.R. Hintz, K. Yolton, K.E. Gustafson, T.M. Leach, C. Green, R. Bara, C.M. Petrie Huitema, R.A. Ehrenkranz, J.E. Tyson, A. Das, J. Hammond, M. Peralta-Carcelen, P.W. Evans, R.J. Heyne, D.E. Wilson-Costello, Y.E. Vaucher, C.R. Bauer, A.M. Dusick, I. Adams-Chapman, R.F. Goldstein, R. Guillet, L.A. Papile, R.D. Higgins, N.N.R.N. Eunice Kennedy Shriver, Childhood outcomes after hypothermia for neonatal encephalopathy, N. Engl. J. Med. 366 (22) (2012) 2085–2092.
[5] U.S. Bhalala, R.C. Koehler, S. Kannan, Neuroinflammation and neuroimmune dysregulation after acute hypoxic-ischemic injury of developing brain, Front. Pediatr. 2 (2014) 144.
[6] H. Hagberg, P. Gressens, C. Mallard, Inflammation during fetal and neonatal life: implications for neurologic and neuropsychiatric disease in children and adults, Ann. Neurol. 71 (4) (2012) 444–457.
[7] H. Hagberg, C. Mallard, D.M. Ferriero, S.J. Vannucci, S.W. Levison, Z.S. Vexler, P. Gressens, The role of inflammation in perinatal brain injury, Nat. Rev. Neurol. 11 (4) (2015) 192–208.
[8] S. Rivest, Regulation of innate immune responses in the brain, Nat. Rev. Immunol. 9 (6) (2009) 429–439.
[9] C. Kaur, E.A. Ling, Periventricular white matter damage in the hypoxic neonatal brain: role of microglial cells, Prog. Neurobiol. 87 (4) (2009) 264–280.
[10] T. Umekawa, A.M. Osman, W. Han, T. Ikeda, K. Blomgren, Resident microglia, rather than blood-derived macrophages, contribute to the earlier and more pronounced inflammatory reaction in the immature compared with the adult hippocampus after hypoxia-ischemia, Glia 63 (12) (2015) 2220–2230.
[11] H. Shen, X. Hu, C. Liu, S. Wang, W. Zhang, H. Gao, R.A. Stetler, Y. Gao, J. Chen, Ethyl pyruvate protects against hypoxic-ischemic brain injury via anti-cell death and anti-inflammatory mechanisms, Neurobiol. Dis. 37 (3) (2010) 711–722.
[12] M. Tang, H. Alexander, R.S. Clark, P.M. Kochanek, V.E. Kagan, H. Bayir, Minocycline reduces neuronal death and attenuates microglial response after pediatric asphyxial cardiac arrest, J. Cereb. Blood Flow Metab. Off. J. Int. Soc. Cereb. Blood Flow and Metab. 30 (1) (2010) 119–129.
[13] K.S. Tang, J.S. Tan, The protective mechanisms of polydatin in cerebral ischemia, Eur. J. Pharmacol. 842 (2019) 133–138.
[14] N. Singh, M. Agrawal, S. Dore, Neuroprotective properties and mechanisms of resveratrol in in vitro and in vivo experimental cerebral stroke models, ACS Chem. Neurosci. 4 (8) (2013) 1151–1162.
[15] Q. He, Z. Li, Y. Wang, Y. Hou, L. Li, J. Zhao, Resveratrol alleviates cerebral ischemia/reperfusion injury in rats by inhibiting NLRP3 inflammasome activation through Sirt1-dependent autophagy induction, Int. Immunopharmacol. 50 (2017) 208–215.
[16] M.S. Lopez, R.J. Dempsey, R. Vemuganti, Resveratrol neuroprotection in stroke and traumatic CNS injury, Neurochem. Int. 89 (2015) 75–82.
[17] S. Pan, S. Li, Y. Hu, H. Zhang, Y. Liu, H. Jiang, M. Fang, Z. Li, K. Xu, H. Zhang, Z. Lin, J. Xiao, Resveratrol post-treatment protects against neonatal brain injury after hypoxia-ischemia, Oncotarget 7 (48) (2016) 79247–79261.
[18] H.C. Wang, O. Bloom, M.H. Zhang, J.M. Vishnubhakat, M. Ombrellino, J.T. Che, A. Frazier, H. Yang, S. Ivanova, L. Borovikova, K.R. Manogue, E. Faist, E. Abraham, J. Andersson, U. Andersson, P.E. Molina, N.N. Abumrad, A. Sama, K.J. Tracey, HMG-1 as a late mediator of endotoxin lethality in mice, Science 285 (5425) (1999) 248–251.
[19] J. Tian, A.M. Avalos, S.Y. Mao, B. Chen, K. Senthil, H. Wu, P. Parroche, S. Drabic, D. Golenbock, C. Sirois, J. Hua, L.L. An, L. Audoly, G. La Rosa, A. Bierhaus, P. Naworth, A. Marshak-Rothstein, M.K. Crow, K.A. Fitzgerald, E. Latz, P.A. Kiener, A.J. Coyle, Toll-like receptor 9-dependent activation by DNA-containing immune complexes is mediated by HMGB1 and RAGE (vol 8, pg 487, 2007), Nat. Immunol. 8 (7) (2007) 780.
[20] G.P. Sims, D.C. Rowe, S.T. Rietdijk, R. Herbst, A.J. Coyle, HMGB1 and RAGE in inflammation and cancer, Annu. Rev. Immunol. 28 (2010) 367–388.
[21] S. Lee, Y. Nam, J.Y. Koo, D. Lim, J. Park, J. Ock, J. Kim, K. Suk, S.B. Park, A small molecule binding HMGB1 and HMGB2 inhibits microglia-mediated neuroinflammation, Nat. Chem. Biol. 10 (12) (2014) 1055–1060.
[22] H. Yang, H. Wang, C.J. Czura, K.J. Tracey, The cytokine activity of HMGB1, J. Leukoc. Biol. 78 (1) (2005) 1–8.
[23] M.G. Frank, M.D. Weber, L.R. Watkins, S.F. Maier, Stress sounds the alarmin: the role of the danger-associated molecular pattern HMGB1 in stress-induced neuroinflammatory priming, Brain Behav. Immun. 48 (2015) 1–7.
[24] Y.N. Paudel, M.F. Shaikh, A. Chakraborti, Y. Kumari, A. Aledo-Serrano, K. Aleksovska, M.K.M. Alvim, I. Othman, HMGB1: a common biomarker and potential target for TBI, neuroinflammation, epilepsy, and cognitive dysfunction, Front. Neurosci. 12 (2018) 628.
[25] T. Nakamura, S. Yamada, T. Yoshioka, Brain hypothermic therapy dramatically decreases elevated blood concentrations of high mobility group box 1 in neonates with hypoxic-ischemic encephalopathy, Dis. Markers 35 (5) (2013) 327–330.
[26] J.E. Rice, R.C. Vannucci, J.B. Brierley, The influence of immaturity on hypoxic-ischemic brain-damage in the rat, Ann. Neurol. 9 (2) (1981) 131–141.
[27] M.M. Rabadi, S. Xavier, R. Vasko, K. Kaur, M.S. Goligorksy, B.B. Ratliff, High-mobility group box 1 is a novel deacetylation target of Sirtuin1, Kidney Int. 87 (1) (2015) 95–108.
[28] D. Yao, W.R. Zhang, X. He, J.H. Wang, K.W. Jiang, Z.Y. Zhao, Establishment and identification of a hypoxia-ischemia brain damage model in neonatal rats, Biomed. Rep. 4 (4) (2016) 437–443.
[29] H. Bian, H. Shan, T. Chen, Resveratrol ameliorates hypoxia/ischemia-induced brain injury in the neonatal rat via the miR-96/Bax axis, Child's Nerv. Syst. ChNS Off. J. Int. Soc. Pediatr. Neurosurg. 33 (11) (2017) 1937–1945.
[30] J. Fan, H. Guang, H. Zhang, D. Chen, L. Ding, X. Fan, F. Xue, Z. Gan, Y. Wang, S. Mao, L. Hu, Y. Gong, SIRT1 mediates apelin-13 in ameliorating chronic normobaric hypoxia-induced anxiety-like behavior by suppressing NF-kappaB pathway in mice hippocampus, Neuroscience 381 (2018) 22–34.
[31] R.B. Roome, J.L. Vanderluit, Paw-dragging: a novel, sensitive analysis of the mouse cylinder test, J. Visualized Exp.: JoVE 98 (2015) e52701.
[32] J.R. Lei, X.K. Tu, Y. Wang, D.W. Tu, S.S. Shi, Resveratrol downregulates the TLR4 signaling pathway to reduce brain damage in a rat model of focal cerebral ischemia, Exp. Ther. Med. 17 (4) (2019) 3215–3221.
[33] X. Xu, X. Liu, Y. Yang, J. He, H. Gu, M. Jiang, Y. Huang, X. Liu, L. Liu, Resveratrol inhibits the development of obesity-related osteoarthritis via the TLR4 and PI3K/Akt signaling pathways, Connect. Tissue Res. (2019) 1–12.
[34] J. Sun, M. Zhang, K. Chen, B.D. Chen, Y.Y. Zhao, H. Gong, X. Zhao, R.M. Qi, Suppression of TLR4 activation by resveratrol is associated with STAT3 and Akt inhibition in oxidized low-density lipoprotein-activated platelets, Eur. J. Pharmacol. 836 (2018) 1–10.
[35] D. He, Z. Guo, J.L. Pu, D.F. Zheng, X.F. Wei, R. Liu, C.Y. Tang, Z.J. Wu, Resveratrol preconditioning protects hepatocytes against hepatic ischemia reperfusion injury via toll-like receptor 4/nuclear factor-kappaB signaling pathway in vitro and in vivo, Int. Immunopharmacol. 35 (2016) 201–209.
[36] T. Bonaldi, F. Talamo, P. Scaffidi, D. Ferrera, A. Porto, A. Bachi, A. Rubartelli, A. Agresti, M.E. Bianchi, Monocytic cells hyperacetylate chromatin protein HMGB1 to redirect it towards secretion, EMBO J. 22 (20) (2003) 5551–5560.
[37] R. Kang, R. Chen, Q. Zhang, W. Hou, S. Wu, L. Cao, J. Huang, Y. Yu, X.G. Fan, Z. Yan, X. Sun, H. Wang, Q. Wang, A. Tsung, T.R. Billiar, H.J. Zeh 3rd, M.T. Lotze, D. Tang, HMGB1 in health and disease, Mol. Asp. Med. 40 (2014) 1–116.
[38] J.B. Kim, C.M. Lim, Y.M. Yu, J.K. Lee, Induction and subcellular localization of high-mobility group box-1 (HMGB1) in the postischemic rat brain, J. Neurosci. Res. 86 (5) (2008) 1125–1131.
[39] X.H. Zhang, B.L. Zhang, S.M. Guo, P. Wang, J.W. Yang, Clinical significance of dynamic measurements of seric TNF-alpha, HMGBl, and NSE levels and aEEG monitoring in neonatal asphyxia, Eur. Rev. Med. Pharmacol. Sci. 21 (19) (2017) 4333–4339.
[40] X. Chen, J. Zhang, B. Kim, S. Jaitpal, S.S. Meng, K. Adjepong, S. Imamura, H. Wake, M. Nishibori, E.G. Stopa, B.S. Stonestreet, High-mobility group box-1 translocation and release after hypoxic ischemic brain injury in neonatal rats, Exp. Neurol. 311 (2019) 1–14.
[41] M.G. Frasch, M. Szynkaruk, A.P. Prout, K. Nygard, M. Cao, R. Veldhuizen, R. Hammond, B.S. Richardson, Decreased neuroinflammation correlates to higher vagus nerve activity fluctuations in near-term ovine fetuses: a case for the afferent

cholinergic anti-inflammatory pathway? J. Neuroinflammation 13 (1) (2016) 103.
[42] M. Wu, F. Liu, Q. Guo, Quercetin attenuates hypoxia-ischemia induced brain injury in neonatal rats by inhibiting TLR4/NF-kappaB signaling pathway, Int. Immunopharmacol. 74 (2019) 105704.
[43] P. Zhang, G. Cheng, L. Chen, W. Zhou, J. Sun, Cerebral hypoxia-ischemia increases toll-like receptor 2 and 4 expression in the hippocampus of neonatal rats, Brain and Development 37 (8) (2015) 747–752.
[44] Y. Luo, C. Wang, W.H. Li, J. Liu, H.H. He, J.H. Long, J. Yang, X. Sui, S. Wang, Z. You, Y.A. Wang, Madecassoside protects BV2 microglial cells from oxygen-glucose deprivation/reperfusion-induced injury via inhibition of the toll-like receptor 4 signaling pathway, Brain Res. 1679 (2018) 144–154.
[45] S. Lehnardt, L. Massillon, P. Follett, F.E. Jensen, R. Ratan, P.A. Rosenberg, J.J. Volpe, T. Vartanian, Activation of innate immunity in the CNS triggers neurodegeneration through a Toll-like receptor 4-dependent pathway, Proc. Natl. Acad. Sci. USA 100 (14) (2003) 8514–8519.
[46] J.R. Caso, J.M. Pradillo, O. Hurtado, P. Lorenzo, M.A. Moro, I. Lizasoain, Toll-like receptor 4 is involved in brain damage and inflammation after experimental stroke, Circulation 115 (12) (2007) 1599–1608.
[47] C.X. Cao, Q.W. Yang, F.L. Lv, J. Cui, H.B. Fu, J.Z. Wang, Reduced cerebral ischemia-reperfusion injury in Toll-like receptor 4 deficient mice, Biochem. Biophys. Res. Commun. 353 (2) (2007) 509–514.
[48] M.M. Buchanan, M. Hutchinson, L.R. Watkins, H. Yin, Toll-like receptor 4 in CNS pathologies, J. Neurochem. 114 (1) (2010) 13–27.
[49] X. Yang, S. Xu, Y. Qian, Q. Xiao, Resveratrol regulates microglia M1/M2 polarization via PGC-1alpha in conditions of neuroinflammatory injury, Brain Behav. Immun. 64 (2017) 162–172.
[50] T. Dragone, A. Cianciulli, R. Calvello, C. Porro, T. Trotta, M.A. Panaro, Resveratrol counteracts lipopolysaccharide-mediated microglial inflammation by modulating a SOCS-1 dependent signaling pathway, Toxicol. In Vitro Int. J. Published Assoc. BIBRA 28 (6) (2014) 1126–1135.
[51] S. Carloni, G. Riparini, G. Buonocore, W. Balduini, Rapid modulation of the silent information regulator 1 by melatonin after hypoxia-ischemia in the neonatal rat brain, J. Pineal Res. 63 (3) (2017).
[52] D. Cao, M. Wang, X. Qiu, D. Liu, H. Jiang, N. Yang, R.M. Xu, Structural basis for allosteric, substrate-dependent stimulation of SIRT1 activity by resveratrol, Genes Dev. 29 (12) (2015) 1316–1325.
[53] M.T. Borra, B.C. Smith, J.M. Denu, Mechanism of human SIRT1 activation by resveratrol, J. Biol. Chem. 280 (17) (2005) 17187–17195.
[54] Y. Matsuzawa-Ishimoto, Y. Shono, L.E. Gomez, V.M. Hubbard-Lucey, M. Cammer, J. Neil, M.Z. Dewan, S.R. Lieberman, A. Lazrak, J.M. Marinis, A. Beal, P.A. Harris, J. Bertin, C. Liu, Y. Ding, M.R.M. van den Brink, K. Cadwell, Autophagy protein ATG16L1 prevents necroptosis in the intestinal epithelium, J. Exp. Med. 214 (12) (2017) 3687–3705.
[55] U.H. Beier, L. Wang, T.R. Bhatti, Y. Liu, R. Han, G. Ge, W.W. Hancock, Sirtuin-1 targeting promotes Foxp3+ T-regulatory cell function and prolongs allograft survival, Mol. Cell. Biol. 31 (5) (2011) 1022–1029.
[56] H. Ding, H. Zhang, H. Ding, D. Li, X. Yi, X. Ma, R. Li, M. Huang, X. Ju, Transplantation of placenta-derived mesenchymal stem cells reduces hypoxic-ischemic brain damage in rats by ameliorating the inflammatory response, Cell. Mol. Immunol. 14 (8) (2017) 693–701.
[57] S. Nikseresht, F. Khodagholi, A. Ahmadiani, Protective effects of ex-527 on cerebral ischemia-reperfusion injury through necroptosis signaling pathway attenuation, J. Cell. Physiol. 234 (2) (2019) 1816–1826.
[58] C. Chang, Y. Zhao, G. Song, K. She, Resveratrol protects hippocampal neurons against cerebral ischemia-reperfusion injury via modulating JAK/ERK/STAT signaling pathway in rats, J. Neuroimmunol. 315 (2018) 9–14.
[59] G. Cheng, X. Zhang, D. Gao, X. Jiang, W. Dong, Resveratrol inhibits MMP-9 expression by up-regulating PPAR alpha expression in an oxygen glucose deprivation-exposed neuron model, Neurosci. Lett. 451 (2) (2009) 105–108.
[60] Y. Shi, X. Guo, J. Zhang, H. Zhou, B. Sun, J. Feng, DNA binding protein HMGB1 secreted by activated microglia promotes the apoptosis of hippocampal neurons in diabetes complicated with OSA, Brain Behav. Immun. 73 (2018) 482–492.
[61] Q. Zhang, L. Yuan, Q. Zhang, Y. Gao, G. Liu, M. Xiu, X. Wei, Z. Wang, D. Liu, Resveratrol attenuates hypoxia-induced neurotoxicity through inhibiting microglial activation, Int. Immunopharmacol. 28 (1) (2015) 578–587.
[62] J.Y. Choi, Y. Cui, S.T. Chowdhury, B.G. Kim, High-mobility group box-1 as an autocrine trophic factor in white matter stroke, P Natl Acad Sci USA 114 (25) (2017) E4987–E4995.
[63] S.A. Back, White matter injury in the preterm infant: pathology and mechanisms, Acta Neuropathol. 134 (3) (2017) 331–349.
[64] S. Calogero, F. Grassi, A. Aguzzi, T. Voigtlander, P. Ferrier, S. Ferrari, M.E. Bianchi, The lack of chromosomal protein Hmg1 does not disrupt cell growth but causes lethal hypoglycaemia in newborn mice, Nat. Genet. 22 (3) (1999) 276–280.
[65] K. Hayakawa, L.D. Pham, Z.S. Katusic, K. Arai, E.H. Lo, Astrocytic high-mobility group box 1 promotes endothelial progenitor cell-mediated neurovascular remodeling during stroke recovery, Proc. Natl. Acad. Sci. U. S. A. 109 (19) (2012) 7505–7510.
[66] X.R. Chen, S.K. Wu, C.N. Chen, B.Y. Xie, Z.N. Fang, W.P. Hu, J.Y. Chen, H.D. Fu, H.F. He, Omega-3 polyunsaturated fatty acid supplementation attenuates microglial-induced inflammation by inhibiting the HMGB1/TLR4/NF-kappa B pathway following experimental traumatic brain injury, J. Neuroinflammation (2017) 14.